LANGMUIR APPLICATIONS LIST - [LP16]

LANGMUIR PROBE SYSTEM

The Impedans' Langmuir Probe system is used by academia and industry globally for plasma characterisation. Below is a list of publications with their plasma sources, process gases, pressures and applications. There are over 130 publications now available in total, watch this space for the complete list.

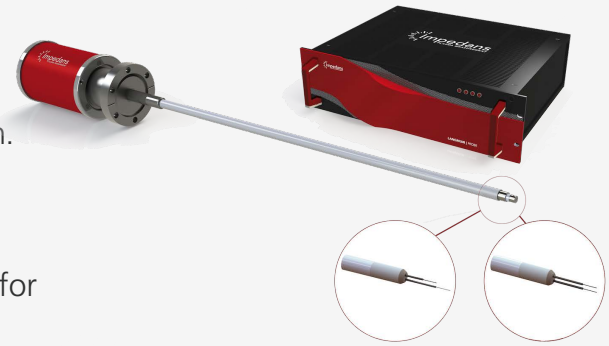

Plasma Source	Density (m^{-3})	Gas	Pressure(mTorr)	Published Paper
2.45GHz Surface Wave	10^{11} -> 10^{15}	N_2 ,N_2/O_2	6000	Electrical characterization of the flowing afterglow of N2 and N2/O2 microwave plasmas at reduced pressure
CCP	10^{14} -> 10^{15}	Ar+C	11.3	Suppression of a spontaneous dust density wave by a modulation of ion streaming
CCP	10^{15} -> 10^{16}	Ar	60 -> 400	Plasma parameters of RF capacitively coupled discharge comparative study between a plane cathode and a large hole
CCP	10^{16}	-	<75	Analysis of double-probe characteristics in low-frequency gas discharges and its improvement
CCP	10^{15}	N_2	100 -> 1000	Capacitively coupled radio frequency nitrogen plasma generated at two different exciting frequencies of 13.56 MHz and 40 MHz
CCP	10^{16} -> 10^{17}	Ar	200 -> 500	Plasma parameters in 40 MHz Argon discharge
Hall Thruster	10^{15} -> 10^{18}	Xe	13.5 -> 45	Anode geometry influence on LaB6 cathode discharge characteristics
Hall Thruster	10^{15} -> 10^{16}	Ar	30	Measurement of plasma parameters in the far-field plume of a Hall effect thruster
Hall Thruster	10^{16} -> 10^{17}	Xe	0.0015	Electron flow properties in the far-field plume of a Hall thruster
Hall Thruster	10^{15} -> 10^{16}	Xe,Kr	0.0225	Time-resolved measurement of plasma parameters in the far-field plume of a low-power Hall effect thruster
Hall Thruster	10^{16}	Xe	0.015	The time-varying electron energy distribution function in the plume of a Hall thruster
Hall Thruster	10^{16} -> 10^{18}	Xe	0.015	Electron energy distribution function in a low-power Hall thruster discharge and near-field plume
Helicon	10^{16} -> 10^{17}	Ar	2.6	Two density peaks in low magnetic field helicon plasma
Helicon	10^{15} -> 10^{16}	Ar	2.62	Modulation of absorption manner in helicon discharges by changing profile of low axial magnetic field*
HiPIMS	10^{16} -> 10^{17}	Ar,Cr	0.5 -> 20	Spectroscopic investigation on the near-substrate plasma characteristics of chromium HiPIMS in low density discharge
HiPIMS	10^{13} -> 10^{17}	Ar,O_2,Ti	6.98	The behaviour of negative oxygen ions in the afterglow of a reactive HiPIMS discharge
HiPIMS	10^{16} -> 10^{18}	Ar,O_2,Ti	5.63	Design of magnetic field configuration for controlled discharge properties in highly ionized plasma
HiPIMS	10^{15} -> 10^{16}	Ar,O_2,Al	1.5	Investigating the plasma parameters and discharge asymmetry in dual magnetron reactive high power impulse magnetron sputtering discharge with Al in Ar/O2 mixture

HiPIMS	10^{16} -> 10^{17}	Ar,O_2,Ti	7.5	Angular dependence of plasma parameters and film properties during high power impulse magnetron sputtering for deposition
HiPIMS	10^{16} -> 10^{18}	Ar,O_2,Ti	5.63	Enhanced oxidation of TiO2 films prepared by high power impulse magnetron sputtering running in metallic mode
HiPIMS - ECWR	< 10^{18}	Ar,O_2,Ti	0.6 -> 75	Deposition of rutile (TiO2) with preferred orientation by assisted high power impulse magnetron sputtering
HiPIMS - ECWR	10^{16} -> 10^{18}	Ar,Ti	0.375	Plasma diagnostics of low pressure high power impulse magnetron sputtering assisted by electron cyclotron wave resonance plasma
Hot Cathode Magnetic Filter	10^{11} -> 10^{12}	Ar,SF_6	0.165	Sheath characteristics in a magnetically filtered low density low temperature multicomponent plasma with negative ions
Hot Cathode Plasma	10^{13}	Ar	0.8	Matched dipole probe for magnetized low electron density laboratory plasma diagnostics
Hot Cathode Plasma	10^{12} -> 10^{13}	Ar	0.15	Ion and electron sheath characteristics in a low density and low temperature plasma
Hybrid – Dual- HiPIMS	10^{17} -> 10^{18}	Ar,Ti,Cu	3 -> 30	Time-resolved Langmuir probe investigation of hybrid high power impulse magnetron sputtering discharges
ICP	10^{17}	H	3.75 -> 22.5	Investigation of the power transfer efficiency in a radio-frequency driven negative hydrogen ion source
ICP	10^{17} -> 10^{18}	Ar	3.75 -> 75	Nonlocal electron kinetics and spatial transport in radio-frequency two-chamber inductively coupled plasmas with argon
ICP	10^{16} -> 10^{17}	Ar,	10 -> 50	A hybrid model of radio frequency biased inductively coupled plasma discharges: description of model and experimental validation in argon
ICP	10^{16} -> 10^{17}	Ar,O_2	10 -> 50	Experimental and numerical investigations on time-resolved characteristics of pulsed inductively coupled O2/Ar plasmas
ICP	10^{15}-> 10^{17}	H,Ar	2 -> 150	Investigation of a Magnetically Enhanced Inductively Coupled Negative Ion Plasma Source
Magnetic Mirror	10^{16}-> 10^{17}	N_2	0.2 -> 4	Signatures of ring currents in a magnetic mirror plasma experiment
Magnetron	10^{16}-> 10^{17}	Ar,Cu	0.75 -> 37.5	The erosion groove effects on RF planar magnetron sputtering
Magnetron	2 -> 70 A/m^2	Ar,N_2,Al	3.75	Tunable ion flux density and its impact on AlN thin films deposited in a confocal DC magnetron sputtering system
MAGPIE	10^{16} -> 10^{17}	Ar	1.4 -> 3	Plasma parameters and electron energy distribution functions in a magnetically focused plasma.
MAGPIE	10^{16} -> 10^{17}	H	5 -> 10	Negative hydrogen ion production in a helicon plasma source
MAGPIE	< 10^{19}	H	10	Ion flux dependence of atomic hydrogen loss probabilities on tungsten and carbon surfaces
MW	10^{14}	Ar	150 -> 200	Apparatus for generating quasi-free-space microwave-driven plasmas
NExET	10^{18}	Xe	-	Anode position influence on discharge modes of a LaB6 cathode in diode configuration
PEGASES Thruster	10^{18}	SF_6,Ar,Xe, He,O_2,N_2	0.75	Plasma drift in a low-pressure magnetized radio frequency discharge
Proton Linear Accelerator	10^{18} -> 10^{19}	H	1.125 -> 5	Plasma characterization of the superconducting proton linear accelerator plasma generator using a 2 MHz compensated Langmuir probe
Pulsed Laser Deposition	10^{16}	O_2,WO_3	7.5	Optimization of substrate-target distance for pulsed laser deposition of tungsten oxide thin films using Langmuir probe
Pulsed Laser Deposition	10^{16} -> 10^{17}	O_2,CeO_2	7.5	Plasma plume behavior of laser ablated cerium oxide: Effect of oxygen partial pressure
PULVA reactor	10^{15}	Ar,C_2H_2	15 -> 30	Metastable argon atom density in complex argon/acetylene plasmas determined by means of optical absorption and emission spectroscopy
VHF Multi-tile Push-Pull	10^{16} -> 10^{17}	N_2	5 -> 25	Nitriding process for next-generation semiconductor devices by VHF (162 MHz) multi-tile push-pull plasma source

*Click here to read more about Langmuir Probe System

Impedans Ltd

Chase House

City Junction Business Park, Northern Cross

Dublin - D17 AK63, Ireland

Tel: +353 1 842 8826

Email: sales@impedans.com

www.impedans.com